Desalination and Water Treatment
www.deswater.com

doi: 10.1080/19443994.2012.749024

51 (2013) 2564–2574
March

Taylor & Francis
Taylor & Francis Group

Evaluation of grinding Salix leaves (gsl) as new sorbent material

I.M. El-Dien[a], A.A. Al-Sarawy[b], M.M. El-Halwany[b,*], A.A. Badawy[a]

[a]*Faculty of Science, Chemistry Department, Port Said University, Egypt*
[b]*Faculty of Engineering, Mathematical and Physical Engineering Department, Mansoura University, Egypt*
Tel. +20 198626614; email: MMelhalwany@mans.edu.eg

Received 15 August 2011; Accepted 2 October 2012

ABSTRACT

Methylene blue (MB) in aqueous solutions was subjected to color removal by the adsorption technique onto grinding Salix leaf (GSL) as agricultural material. Results obtained indicate that the removal efficiency of MB at 30˚C reaches 99% and that the adsorption process is highly pH-dependent. The results fit Langmuir model adsorption of MB on GSL, verify the assumption that the adsorbate molecules could be adsorbed in one layer thick on the surface of the adsorbent. A comparison of kinetic at different conditions showed that the pseudo-second-order kinetic model correlates the experimental data well. van't Hoff equation was used to evaluate the thermodynamic parameters (ΔH, ΔS, and ΔG), which indicate that all adsorption processes are exothermic, and this is agreement with the stability of adsorption capacity with temperature, chemically in nature, and spontaneous.

Keywords: Adsorption; Isotherms; Kinetic models; Salix leaves; Thermodynamic parameters

1. Introduction

Contamination of surface and ground water with synthetic dyes is serious environmental problem that causes threat to human being and aquatic life. Colored wastewater is an important environmental problem, as it impedes light penetration and retards the photosynthesis, increase COD and BOD levels of aquatic sources [1]. Due to their aromatic structure and synthetic origin, most of the dyes are stable to the photodegradation and biodegradation. Among the techniques employed for the scavenging the dyes are chemical precipitation, adsorption, ion exchange, photodegradation, biodegradation, membrane filtration, and reverse osmosis [2].

Often when one envisions a quiet body of water, the graceful, elegant form of a Weeping Willow is seen at the water's edge, the long, light green, pendulous branches reflected in the water, gently swaying with each little breeze. Though it does well in very moist soils, Weeping Willows may also be successfully used as a fast-growing specimen or screen in drier, more open areas where it should receive regular watering to prevent leaf drop in a drought. It will survive drought but loses some leaves without irrigation. Ultimately reaching a height of 35–45 feet with an equal or greater spread, Weeping Willow should be given plenty of room to develop its broad, rounded crown [3].

Synthetic dyes are widely used in various industries such as textile, leather, paper, printing, food, cosmetics, paint, pigments, petroleum, solvent, rubber, plastic, pesticide, wood preserving chemicals, and pharmaceutical industry. Over 10,000 of different com-

*Corresponding author.

mercial dyes and pigments exist and more than 7×10^5 tonnes are produced annually worldwide. Approximately 12% of synthetic dyes are lost during manufacturing and processing operations and 20% of these lost dyes enter the industrial wastewaters. Textile industries consume two-thirds of the dyes manufactured. During textile processing, up to 50% of the dyes are lost after the dyeing process and about 10–15% of them are discharged in the effluents. The textile manufacturing industry alone discharges about 1,46,000 tonnes of dyes per year along with its wastewater which ultimately finds its way into the environment. Generally the wastewater contains dye concentrations ranging from 10 to 200 mg L^{-1}. The discharge of dye containing effluents into the natural water bodies can pose hazardous effects on the living systems because of carcinogenic, mutagenic, allergenic, and toxic nature of dyes. Dyes impede light penetration, retard photosynthetic activity, inhibit the growth of biota, and also have a tendency to chelate metal ions which result in microtoxicity to fish and other organisms [4].

Cationic dyes such as MB, a thiazine, were used initially for dyeing of silk, leather, plastics, paper, and cotton mordant with tannin, as well as for the production of ink and copying paper in the office supplies industry [5]. In the textile sector, an estimated 10–20% of dyes (active substance) used is lost in residual liquors through the exhaustion and washing operations [6]. The releasing of dyes to the environment can cause acute and/or chronic effects on the exposed organisms, adsorb or reflect sunlight entering into water, and thus result in change of food chain [7].

Previous studies found that MB molecules existed as dimers or as aggregates at the surface, as well as a protonated form depending on the concentration and the surface properties [8]. Such extensive use of dyes and pigments often poses problems in the form of colored wastewater that require pretreatment for color removal prior to disposal into receiving water bodies or publicly owned treatment works [9]. The main problem for dyestuff manufacturers and users is the removal or reducing the quantity of color in effluent and water sources [10].

Although methylene blue (MB) is not hazardous compared to other commercial dyes, acute exposure to MB can cause increased heart rate, vomiting, diarrhea, nausea, and shock. It can cause eye burns, which may be responsible for permanent injury to the eyes of human and on inhalation, it can give rise to short periods of rapid or difficult breathing, whereas ingestion through mouth produces a burning sensation. Potential exposure to MB can also cause hypertension, precordial pain, dizziness, headache, fever, fecal discoloration, profuse sweating, mental confusion, methemoglobinemia, and hemolytic anemia. Hence, there is a necessity for the treatment of effluent containing such dye due to its harmful impacts on receiving waters [11].

At the present time there is no single process capable of adequate treatment [12]. Most of the existing processes include adsorption, usually with activated carbon (AC) [13]. The adsorption of the cationic dye, MB, has been used for a long time for the evaluation of the adsorption properties of AC, and in monitoring the production and quality of AC prepared from coal, in fluidized bed [14]. Adsorption from dilute aqueous solutions onto solid surfaces is a highly attractive separation technique for many applications, such as wastewater treatment, liquid mixture separation, and purification, or polar organic solutes recovery from biotechnology processes [15,16]. In particular, adsorption provides a technique of great interest to remove dyes from municipal and industrial wastewater [17,18]. This can be achieved by using adsorbents with a high adsorptive capacity [19].

The adsorption process can be either physical or chemical in nature, and frequently involves both. Physical adsorption involves the attraction by electrical charge differences between adsorbent and the adsorbate. Chemical adsorption is the product of a reaction between the adsorbent and the adsorbate [20]. In recent years, stringent government regulations have made it mandatory to stop such effluents, unless they are treated properly; hence, the removal of color from the effluent discharge has become environmentally important [21,22].

2. Materials and methods

2.1. Preparation of GSL

Salix leaves were lightly ground in a mortar, then immersed in distilled water for 24 h, and then dried in a drier at 105°C to remove the yellow color of the extract. The dried GSL sieved through 0.5 and 0.08 mm diameter by means of a test sieve shaker.

2.2. Batch adsorption studies

Batch experiments with GSL were conducted to investigate the initial adsorbent particle size (<0.08, 0.08–0.1, 0.1–0.125, 0.125–0.16, and 0.16–0.315 mm), adsorbent dose (0.6, 1, 1.6, 3, and 3.6 gm), 50 ml volume of dye concentration (25, 50, 75, 100, and 125 mg L^{-1}), adsorption time (10, 20, 25, 30, 35, and 40 min), pH (2, 5, 7.5, 9, and 12), and temperature (30, 40, 50, and 60°C) on MB adsorption. All reagents used were of AR grade

(Sigma–Aldrich, Germany). MB stock solution was prepared by dissolving a known amount of the dye in distilled water and diluted to the required initial concentration. About 50 ml of MB solution of known concentration (c_o) was taken in a 100 ml conical flask with the required amount of adsorbent and kept under shaking for different time intervals in a shaker at different pH values and different temperatures. Then, the solution was filtered through a filter paper. UV–visible spectrophotometer (model PHTOMECH 301-D$^+$, λ_{max}: up to 1200, made in German) was employed to determine the remaining concentrations of MB in the filtrate at 670 nm. All adsorption experiments were performed in triplicate, and the mean values were used in data analysis. Blank experiments, performed without the addition of adsorbent, confirmed that the sorption of dye on the walls of flasks was negligible. The details of the dye used are given in Table 1 and the structure is shown below.

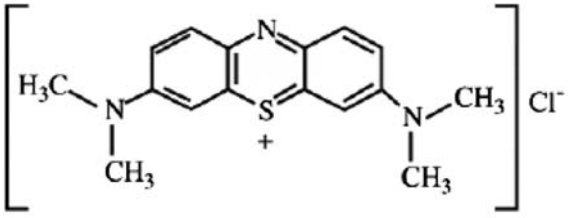

Methylene Blue (MB) structure.

3. Adsorption isotherms study

The main factors that play the key role for the dye–adsorbent interactions are charge and structure of dye, adsorbent surface properties, hydrophobic and hydrophilic nature, hydrogen bonding, electrostatic interaction, steric effect, van der Waal forces, etc. [23]. Equilibrium studies that give the capacity of the adsorbent and adsorbate are described by adsorption isotherms, which is usually the ratio between the quantity adsorbed and that remained in solution at equilibrium at fixed temperature. Freundlich, Langmuir, and BET (Brunauer, Emmett, and Teller) isotherms are the earliest and simplest known relationships describing the adsorption equation [24,25].

Table 1
Properties of methylene blue (MB)

Molecular weight	319.85222 [g/mol]
Molecular formula	$C_{16}H_{18}ClN_3S$
λ_{max}	670 nm
Odor	Slight odor
Melting point	105 °C (decomposes)
IUPAC name	3,7-bis(dimethylamino) phenazathionium chloride, tetramethylthionine chloride
Commercial name	Methylene blue, thiazine
Covalently bonded unit count	2
H-bond donor	0
H-bond acceptor	3
Water solutions	Deep blue
Solubility in water	43,600 mg/L at 25 °C
Vapor pressure	1.30×10^{-7} mm Hg at 25 °C
Henry's constant	1.25×10^{-12} atm m^3/mol at 25 °C

Fig. 1. Cross-sections through the leaf of *Salix*.

3.1. Langmuir Isotherm

The Langmuir equation is used to estimate the maximum adsorption capacity corresponding to complete monolayer coverage on the adsorbent surface and is expressed by:

$$q_e = (q_{max} K_L C_e)/(1 + K_L C_e) \quad (1)$$

The linearise form of the above equation after rearrangement is given by:

$$C_e/q_e = 1/q_{max} K_L + C_e/q_{max} \quad (2)$$

The experimental data is then fitted into the above equation for linearization by plotting C_e/q_e against C_e.

3.2. Freundlich isotherm

The Freundlich model named after Freundlich (1926) is an empirical equation used to estimate the

adsorption intensity of the sorbent towards the adsorbate and is given by:

$$q_e = K_F C_e 1/n \quad (3)$$

Also, the value of n indicates the affinity of the adsorbate towards the adsorbent. The above equation is conveniently used in linear form as:

$$\ln q_e = \ln K_F + (1/n) \ln C_e \quad (4)$$

A plot of $\ln C_e$ against $\ln q_e$ yielding a straight line indicates the conformation of the Freundlich adsorption isotherm. The constants $1/n$ and $\ln K_F$ can be determined from the slope and intercept, respectively.

3.3. BET isotherm

The BET derived an adsorption isotherm based on the assumption that the adsorbate molecules could be adsorbed in more than one layer thick on the surface of the adsorbent. Their equation, like langmuir equation, assumes that the adsorbent surface is composed of uniform, localized sites and that the adsorption at one site does not affect adsorption at neighboring sites. Moreover, it was assumed that the energy of adsorption holds the first monolayer but that the condensation energy of the adsorbate is responsible for adsorption of successive layers. The equation, known as the BET equation, is commonly written as follow:

$$x/m = AcX_m/(c_s - c)\,[1 + (A-1)c/c_s] \quad (5)$$

Rearranging the BET equation yields:

$$C/(C_s - C)x/m = 1/AX_m + (A-1)(C/C_s)/AX_m \quad (6)$$

Thus, plotting $C/(C_s - C)$ against C/C_s will give rise to straight lines with slope $(A-1)/AX_m$ and intercept $1/AX_m$ for adsorption processes that conform BET equation [26].

4. Adsorption dynamics study

The study of adsorption dynamics describes the solute uptake rate and evidently this rate controls the residence time of adsorbate uptake at the solid–solution interface. Kinetics of (MB) adsorption on the GSL was analyzed using pseudo-first-order, pseudo-second-order, Elovich, and intraparticle diffusion kinetic models [27].

4.1. The pseudo-first-order model

The pseudo-first-order equation (Lagergren, 1898) is generally expressed as follows:

$$\frac{dq_t}{dt} = k_1(q_e - q_t) \quad (7)$$

At $t = 0$ to $t = t$ and $q_t = 0$ to $q_t = q_t$, the integrated form of Eq. (7) becomes:

$$(\log q_e - \log q_t) = \log(q_e) - \frac{k_1}{2.303} t \quad (8)$$

where k_1 and q_e can be determined from the slope and intercept of the plot.

4.2. The pseudo-second-order model

The pseudo-second-order kinetic rate equation is expressed as (Ho et al., 2000):

$$\frac{dq_t}{dt} = k_2(q_e - q_t)^2 \quad (9)$$

At $t = 0$ to $t = t$ and $q_t = 0$ to $q_t = q_t$, the integrated form of Eq. (9) becomes:

$$\frac{1}{(q_e - q_t)} = \frac{1}{q_e} + kt \quad (10)$$

Eq. (4) can be rearranged to obtain Eq. (11), which has a linear form:

$$\frac{t}{q_t} = \frac{1}{k_2 q_e^2} + \frac{1}{q_e} t \quad (11)$$

If the initial adsorption rate, h (mg/g min) is:

$$h = k_2 q_e^2 \quad (12)$$

then Eq. (11) and (12) become:

$$\frac{t}{q_t} = \frac{1}{h} + \frac{1}{q_e} t \quad (13)$$

The plot of (t/q_t) and t of Eq. (11) should give a linear relationship from which q_e and k_2 can be determined from the slope and intercept of the plot, respectively.

4.3. The Elovich model

The Elovich model equation is generally expressed as:

$$\frac{dq_t}{dt} = \alpha \exp(-\beta q_t) \quad (14)$$

To simplify the Elovich equation, Chien and Clayton (1980) assumed $\alpha\beta t >> t$ and by applying the boundary conditions $t = 0$ to $t = t$ and $q_t = 0$ to $q_t = q_t$, Eq. (14) becomes:

$$q_t = \frac{1}{\beta}\ln(\alpha\beta) + \frac{1}{\beta}\ln(t) \quad (15)$$

A plot of q_t vs. $\ln(t)$ should yield a linear relationship with a slope of $(1/\beta)$ and an intercept of $(1/\beta)$ $\ln(\alpha\beta)$.

4.4. The intraparticle diffusion model

The intraparticle diffusion model is expressed as (Weber and Morris, 1963)

$$R = k_{id}(t)^a \quad (16)$$

A linearized form is obtained as:

$$\log R = \log k_{id} + a \log(t) \quad (17)$$

If (MB) adsorption fits the intraparticle model, a plot of $\log R$ vs. $\log t$ should yield a linear relationship with a slope of a and an intercept of $\log k_{id}$.

5. Results and discussion

5.1. General information of Salix leaf

A cross section through the leaf of Salix and scanning electron micrographs of Salix leaves are shown in Figs. 1 and 2.

5.2. Adsorption isotherms

The results of this study show that GSL was effective, in adsorbing MB as its removal reached 99% at 30 ℃. Adsorption of MB was highly pH-dependent and the results showed that the optimum pH for the removal was found to be (6–8), at which MB exists mostly as the most easily adsorbed form aqueous solution increases as the initial MB concentration. Also smaller adsorbate particle were found to increase the percentage removal of MB, but the increasing of temperature results no changing in the removal efficiency. The experimental data were applied in the three isotherms, where results indicate that the adsorption of MB on GSL fits the Langmuir model (Fig. 3) with

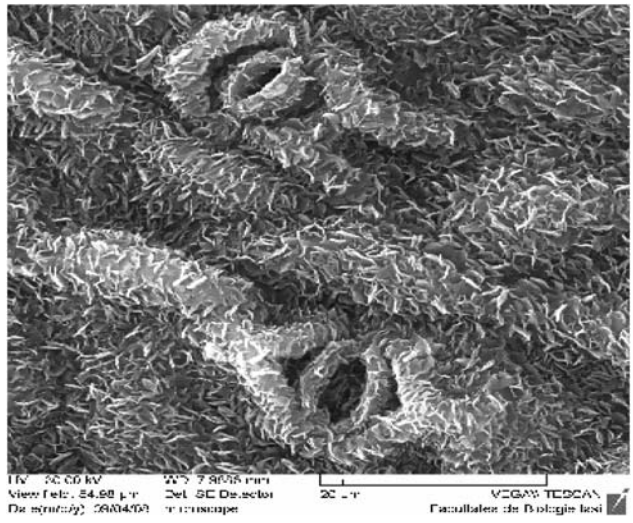

Fig. 2. SEM of *Salix* leaves.

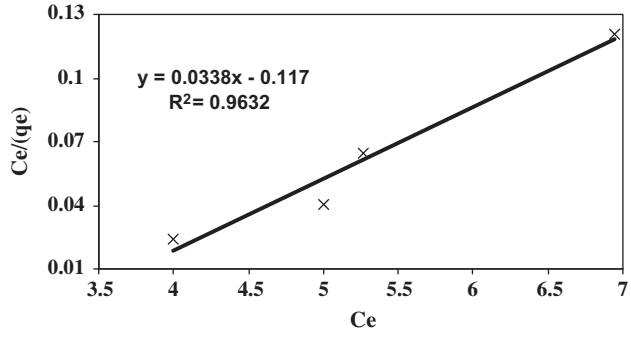

Fig. 3. Langmuir isotherm.

$R^2 = 0.96$, verifying the assumption that the adsorbate molecules could be adsorbed in one layer thick on the surface of the adsorbent.

5.3. Adsorption dynamics

5.3.1. Effect of adsorbate concentrations

The removal of MB was found to increase with time and attained a maximum value at 40 min. On changing the initial concentration of MB solution from 25 to 125 mg/l, the amount adsorbed increased at 25° C, pH 7.5, and particle size of 0.08 mm. As a rule, increasing the initial dye concentration results in an increase in the adsorption capacity because it provides a driving force to overcome all mass transfer resistances of dyes between the aqueous and solid phase. The experimental results correlate with the theoretically predicted curves. Results obtained show good compliance with the pseudo-second-order kinetic model (Fig. 4).

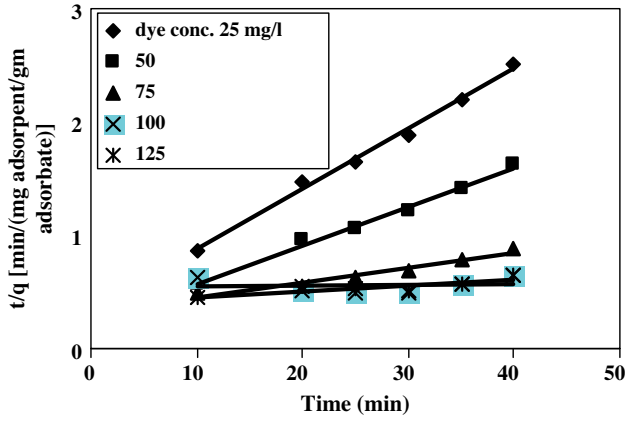

Fig. 4. Pseudo-second-order equation at different adsorbate concentrations.

5.3.2. Effect of adsorbent particle size

The removal of MB increased with the decrease in particle size. The relatively higher adsorption with smaller adsorbent particle may be attributed to the fact that smaller particles yield large surface areas. The data obtained separately for each of the kinetic models from the slopes of plots, show a good compliance with pseudo-second-order equation (Fig. 5).

5.3.3. Effect of temperature

Equilibrium capacity can be changed by temperature of the adsorbent for a particular adsorbate. In our case, the experimental data which obtained at pH 7.5, particle size blew 0.08 mm, and initial concentration of 25 mg/l show that small changing of adsorption capacity at temperature from 30 to 60°C. The small enhancement in adsorption with rise in temperature may be attributed to increase in the number of active surface sites available for adsorption, increase in the porosity, and in the pore volume of the adsorbent. An increase of temperature increases the rate of diffusion of the adsorbate molecules across the external boundary layer and within the internal pores of the adsorbent particle, due to decrease in the viscosity of the solution. The small enhancement in adsorption may also be a result of an increase in the mobility of the dye molecules with an increase in their kinetic energy. The data obtained for each of the kinetic models from the slopes of plots (Fig. 6) show a good compliance with the pseudo-second-order equation.

5.3.4. Effect of adsorbent dose

MB uptake was studied at pH 7.5, 25°C, particle size below 0.08 mm and initial concentration of 25 mg/l. The concentrations used were 0.5, 0.75, 1, 1.25, and 1.5 g adsorbent/liter adsorbate, keeping the batch experimental volume the same in all cases. The results indicated that the percentage adsorption increased with the increase in GSL dose. It can be explained that the adsorbent has a limited number of active sites and it increase with the increase of the adsorbent dose. The curves (Fig. 7), showed good compliance with pseudo-second-order model.

5.3.5. Effect of pH

The pH of the aqueous solution has been recognized as one of the most important factors influencing any adsorption process. It influences not only the surface charge of the adsorbent, the degree of ionization of the material present in the solution, and the dissociation of functional groups on the active sites of the adsorbent, but also the solution dye chemistry. The removal of MB was studied at different pHs in the

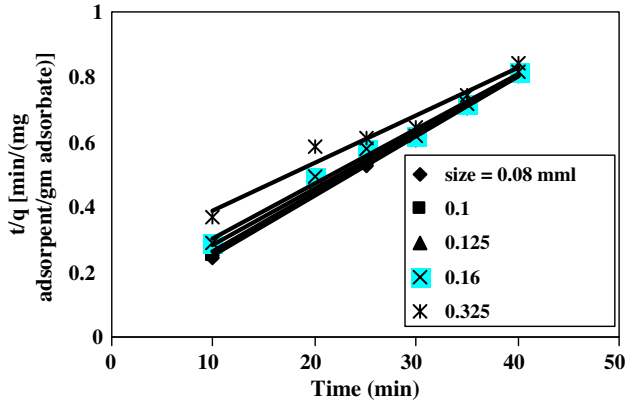

Fig. 5. Pseudo-second-order equation at different adsorbent particle sizes.

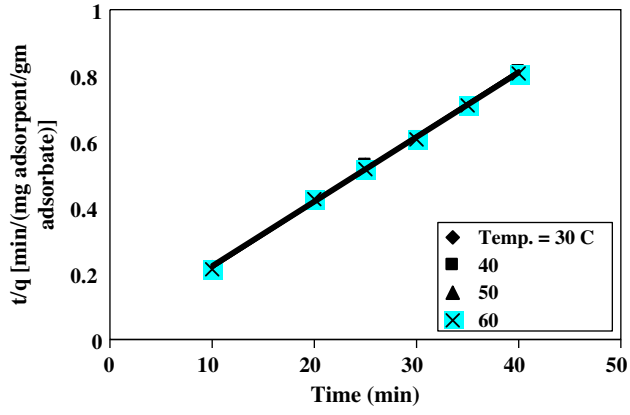

Fig. 6. Pseudo-second-order equation at different temperatures.

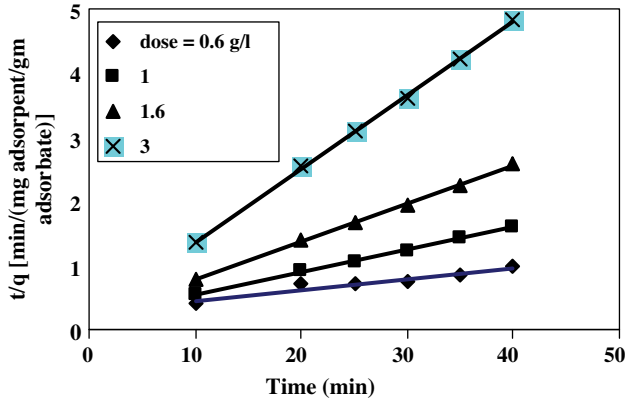

Fig. 7. Pseudo-second-order equation at different adsorbent doses.

range 2–12 by GSL at initial MB concentration of 25 mg/l, a temperature of 25°C, and particle size blew 0.08 mm. The maximum sorption capacity takes place at pH range 6–8 and removal percentage of the dye was 91%. MB is a cationic dye, which exists in aqueous solution in the form of positively charged ions. As a charged species, the degree of its adsorption onto the adsorbent surface is primarily influenced by the surface charge on the adsorbent, which in turn is influenced by the solution pH. At low pH values, the protonation of the functional groups present on the adsorbent surface easily takes place, and thereby restrict the approach of positively charged dye cations to the surface of the adsorbent resulting in low adsorption of dye in acidic solution. With decrease in acidity of the solution, the functional groups on the adsorbent surface become de-protonated resulting in an increase in the negative charge density on the adsorbent surface and facilitate the binding of dye cations. The increase in dye removal capacity at higher pH may also be attributed to the reduction of H^+ ions which compete with dye cations at lower pH for appropriate sites on the adsorbent surface.

However, with increasing pH, this competition weakens and dye cations replace H^+ ions bound to the adsorbent surface resulting in increased dye uptake. Results also showed that the adsorption reaction can be approximated with the pseudo-second-order kinetic model (Fig. 8). The rate constants and values of correlation coefficient are represented in Table 2.

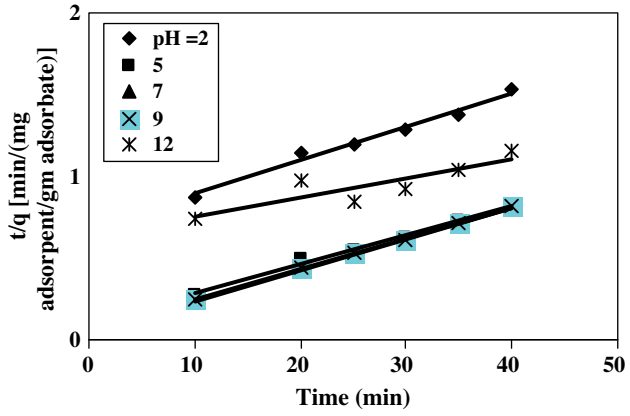

Fig. 8. Plot of pseudo-second-order equation at different pH values.

5.4. Thermodynamic parameters

5.4.1. Determination of ΔH°, ΔS°, and ΔG°

The values of the thermodynamic parameters, enthalpy variation (ΔH) and entropy variation (ΔS), were calculated from the curve relating the distribution coefficient (K_D) as a function of temperature (Fig. 9) using the equation:

$$\ln K_D = \left(\frac{\Delta S^\circ}{R}\right) - \left(\frac{\Delta H^\circ}{RT}\right) \quad (18)$$

where K_D is the distribution coefficient ($cm^3\,g^{-1}$), defined as:

$$K_D = \frac{Q}{C_e} \quad (19)$$

where Q is the amount adsorbed (mg adsorbate/g adsorbent) described by the equation:

$$Q = \frac{V(C - C_e)}{m} \quad (20)$$

where C and C_e are the initial and equilibrium concentrations of the solute, respectively (mg cm^{-3}). The calculated data for K_D and Q are shown in Table 3.

The free energy change (ΔG°) parameter was calculated using Eq. (21):

$$\Delta G^\circ = \Delta H^\circ - T\Delta S^\circ \quad (21)$$

From Fig. 9 the values of ΔH°, ΔS° were determined from the slopes and intercepts of the curves, respectively, as well as the calculated values of ΔG° and are listed in Table 4. Investigation of the obtained values of the thermodynamic parameters shows that the adsorption process is exothermic. This is in accordance with increasing adsorption equilibrium with increasing temperature.

Table 2
The adsorption kinetic model rate constants for GSL

Parameter		First order		Second order				Elovich model		Intraparticle diffusion		
		k_1	r^2	k_2	H	R^2	β	α	r^2	k_{id}	a	r^2
pH	2	0.114	0,876	0.026	1.451	0.982	0.090	2.971	0.986	5.6×10^{30}	51.10	0.986
	5	0.164	0.872	0.156	9.852	0.994	0.112	55.37	0.935	3.96×10^{32}	41.15	0.935
	7.5	0.225	0.905	0.333	20.04	0.999	0.179	1103.7	0.932	8.59×10^{58}	25.66	0.932
	9	0.271	0.831	0.275	16.69	0.999	0.160	456.8	0.950	4.79×10^{53}	28.81	0.951
	12	0.123	0.934	0.017	1.588	0.994	0.061	3.562	0.946	2.6×10^{51}	75.97	0.946
Particle size (mm)	0.08	0.224	0.790	0.228	14.20	0.995	0.147	282.6	0.894	3.9×10^{50}	31.23	0.894
	0.1	0.237	0.777	0.185	11.74	0.991	0.129	125.9	0.864	1.8×10^{43}	35.74	0.864
	0.125	0.240	0.806	0.146	9.416	0.992	0.105	44.96	0.932	4×10^{29}	44.05	0.932
	0.15	0.217	0.804	0.109	7.310	0.989	0.087	21.50	0.949	2.2×10^{14}	53.18	0.949
	0.325	0.160	0.870	0.056	4.212	0.991	0.063	8.382	0.946	6×10^{21}	73.03	0.946
Adsorbent dose (mg/l)	0.6	0.312	0.746	0.053	3.564	0.932	0.073	7.303	0.895	1.6×10^{21}	75.78	0.895
	1	0.291	0.819	0.143	4.885	0.996	0.193	18.02	0.951	6.7×10^{25}	47.62	0.951
	1.6	0.283	0.846	0.252	5.285	0.999	0.477	99.59	0.958	5.9×10^{51}	0.194	0.959
	3	0.240	0.830	0.365	4.272	0.999	1.299	1041.8	0.964	4.3×10^{66}	30.87	0.958
Temp. (°C)	30	0.243	0.811	0.569	33.11	0.999	0.345	1.71×10^{06}	0.889	1.2×10^{77}	13.36	0.889
	40	0.238	0.812	0.745	42.92	0.999	0.459	3.47×10^{08}	0.838	2×10^{82}	10.04	0.838
	50	0.252	0.849	0.711	41.15	0.999	0.404	29.4×10^{06}	0.920	4×10^{80}	11.40	0.920
	60	0.248	0.867	0.827	47.85	0.999	0.480	1.12×10^{09}	0.835	5×10^{83}	0.284	0.950
Concentration (mg/l)	25	0.296	0.850	0.125	2.894	0.994	0.287	9.605	0.949	1×10^{22}	50.07	0.949
	50	0.326	0.872	0.128	4.437	0.992	0.183	14.49	0.931	2×10^{21}	50.17	0.931
	75	0.159	0.891	0.038	3.216	0.939	0.054	6.102	0.959	2×10^{32}	65.67	0.959
	100	0.223	0.876	0.002	1.868	0.920	0.028	5.647	0.970	2.2×10^{76}	95.25	0.970
	125	0.150	0.855	0.012	2.473	0.992	0.032	5.932	0.955	2.6×10^{48}	65.86	0.955

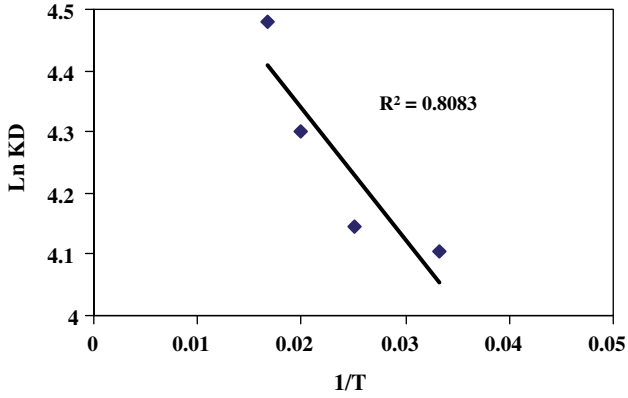

Fig. 9. Plot of K_D vs. 1/T.

Table 3
Q and K_D parameters at different temperatures

Temperature (°C)	Q	K_D
30	49.12	60.642
40	49.22	63.103
50	49.33	73.627
60	49.44	88.286

Table 4
Thermodynamic parameters at different temperatures

ΔH (kcal/mol)	ΔS (kcal/mol K)	ΔG (kcal/mol)			
		30°C	40°C	50°C	60°C
−0.0756	0.367	−111.8	−115.5	−119.2	−122.9

5.4.2. Determination of mean free energy (E)

The mean free energy of adsorption (E) is the free energy change when one mole of ions is transferred to the surface of the membrane from infinity in the solution and it is calculated from:

$$E = -(2K_D R)^{\frac{1}{2}} \quad (22)$$

The mean free energies (E) were calculated and documented in Table 5.

The magnitude of E is useful for estimating the type of sorption reaction, since $E < 8\,\text{kJ mol}^{-1}$, physical forces such as diffusion processes may affect the sorption mechanism [24]. So, the adsorption of dyes seems to be a complex phenomenon, where diffusion and chemical bonding occur at different temperature ranges, this may support that the monolayer capacity (q_{max}) increases with increasing temperature.

Table 5
Free energy (e) at different temperatures

Temperature (°C)	K_D	E, kJ/mol
30	60.64	15.497
40	63.103	15.808
50	73.627	17.075
60	88.29	18.698

Table 6
Comparison between adsorption capacity of low-cost adsorbents

Sorbent	q_{max} (mg g^{-1})	Ref.
Degreased coffee bean	55.3	[28]
Treated sawdust	65.8	[29]
Arundo donax root carbon	8.69	[30]
Activated charcoal	0.179	[31]
Waste apricot	116.27	[32]
Activated carbons commercial grade	8.27	[33]
Laboratory grade activated carbons	42.18	[33]
Bentonite	7.72	[34]
Sugarcane dust	4.88	[35]
Hen feathers	26.1	[36]
Iron humate	19.2	[37]
Rubber wood sawdust	36.45	[38]
Cellulose	2.422	[39]
Neem leaf powder	133.6	[40]
Ricinus communis	27.78	[41]
Lemon peel	51.73	[42]
Caulerpa racemosa var. cylindracea	26.57	[43]
Rattan sawdust	62.7	[44]
Maize cob powder	37.037	[45]
Sea shell powder	42.33	[45]
Salix leaves powder	62.35	Our work

Table 6 shows some of the adsorption capacities of low-cost adsorbents reported in the literature.

6. Conclusion

- The adsorption process fits the Langmuir model, corroborating the assumption that the adsorbate molecules could be adsorbed in mono layer thick on the surface of the adsorbent.
- The kinetics of MB adsorption on the GSL was found to follow a pseudo-second-order rate equation.

- The mean free energies (E) revealed that, adsorption of dyes on GSL seems to be a complex phenomenon, where diffusion and chemical bonding occur at different temperature ranges.
- The values of thermodynamic parameters indicate that all adsorption processes are exothermic, and this is in agreement with the stability of adsorption capacity with temperature.
- Thermodynamic studies are performed and the values of the parameters suggest that the process of removal of MB by GSL is a spontaneous one.

Nomenclature

A	—	constant describing the energy of interaction between solute and adsorbent surface
C	—	initial concentration, mg/l
C_e	—	concentration equilibrium, mg/l
C_s	—	saturation concentration of solute, mg/l
K_F & n	—	Freundlich constants
m	—	mass of adsorbent, mg
k_1	—	rate constant of pseudo-first-order adsorption, l/min
k_2	—	rate constant of pseudo-second-order adsorption, g/mg min
K_D	—	distribution coefficient, $cm^3\ g^{-1}$
k_{id}	—	intraparticle diffusion rate constant, min^{-1}
K_L	—	constant related to the adsorption/desorption energy, $l\ g^{-1}$
q_e	—	adsorption capacity at equilibrium, mg of dye/g adsorbate
q_{max}	—	maximum sorption, mg of dye/g adsorbate
q_t	—	adsorption capacity at time t, mg of dye/g adsorbate
R	—	universal gas constant, j/mole K
R	—	percent (MB) adsorbed
t	—	contact time, min
V	—	volume of the solution
x	—	amount of solute adsorbed, mg
X_m	—	amount of solute adsorbed in forming a complete mono layer, mg of dye/g adsorbate
α	—	initial adsorption rate, mg of dye/g adsorbate min
β	—	desorption constant, g/mg during any experiment

References

[1] A. Rais, K. Rajeev, Synthesis and properties of cellulose carbon encapsulated ZnO for dye removal, J. Disper. Sci. Technol. 32 (2011) 737.

[2] S. Chokarborty, B.C. Bag, S.D. Gupta, S. De, J.K. Basu, Separation and fractionation of dye solution by nanofiltration, Sep. Sci. Technol. 38 (2003) 219.

[3] E.F. Gilman, D.G. Watson, *Salix* spp: Weeping Willow, Fact Sheet ST-576, a series of the Environmental Horticulture Department, University of Florida, 1994.

[4] S. Chowdhury, R. Mishra, P. Saha, P. Kushwaha, Adsorption thermodynamics, kinetics and isosteric heat of adsorption of malachite green onto chemically modified rice husk, Desalination 265 (2011) 159.

[5] H. Berneth, A.G. Bayer, Ullmanns Encyclopedia of Industrial Chemistry, Wiley–VCH Press, Germany, 2003, p. 585.

[6] Z.Z. Shan, L.J. Fu, T. Chao, Z.Q. Fang, H.J. Tian, J.G. Bin, Rapid decolorization of water soluble azo-dyes by nanosized zero-valent iron immobilized on the exchange resin, Sci. China. Ser. B-Chem. 51 (2008) 186.

[7] Y.C. Wong, Y.S. Szeto, W.H. Cheung, Effect of temperature, particle size and percentage deacetylation on the adsorption of acid dyes on chitosan, Adsorption 14 (2008) 11.

[8] K. Fujita, K. Taniguchi, H. Ohno, Dynamic analysis of aggregation of methylene blue with polarized optical waveguide spectroscopy, Talanta 65 (2005) 1066.

[9] P. Waranusantigul, P. Pokethitiyook, M. Kruatrachue, E.S. Upatham, Kinetics of basic dye (Methylene Blue) biosorption by giant duckweed (*Spirodela polyrrhiza*), Environ. Pollut. 125 (2003) 385.

[10] M.F.R. Pereira, S.F. Soares, J.J.M. Orfao, J.L. Figueiredo, Adsorption of dyes on activated carbons: Influence of surface chemical groups, Carbon 41 (2003) 811.

[11] S. Chowdhury, P. Saha, Pseudo-second-order kinetic model for biosorption of methylene blue onto tamarind fruit shell: Comparison of linear and nonlinear methods, Bioremediat. J. 14 (2010) 196.

[12] P. Cooper, Removing colour from dye house wastewaters – a critical review of technology available, J. Soc. Dyers Colour 109 (1993) 97.

[13] U. Rott, R. Minke, Overview of wastewater treatment and recycling in the textile processing industry, Water Sci. Technol. 40 (1999) 137.

[14] S.S. Barton, the adsorption of methylene blue by active carbon, Carbon 25 (1987) 343.

[15] C.M. GonzaAlez-Garcia, R. Denoyel, M.L.G. Martin, V.G. Serrano, Influence of porosity on the adsorption enthalpies of a non-ionic surfactant onto carbonaceous materials, Thermochim. Acta 375 (2001) 177.

[16] L.K. Wang, R.P. Leonard, M.H. Wang, D.W. Goupil, Adsorption of dissolved organics from industrial effluents on to activated carbon, J. Appl. Chem. Biotechnol. 25 (1975) 491.

[17] A.I. Zouboulis, K.A. Matis, The biosorption process: An innovation in reclamation of toxic metals, In: G.P. Gallios, K.A. Matis (Eds), Mineral Processing and the Environment, Kluwer Academic, Dordrecht, p. 361, 1998.

[18] H. Weinberg, N. Narkis, Physico-Chemical treatments for the complete removal of non-ionic surfactants from effluents, Environ. Pollut. 45 (1987) 245.

[19] O. Dusart, S. Souabi, M. Mazet, Elimination of surfactants in water treatment by adsorption onto activated carbon, Environ. Technol. 11 (1990) 721.

[20] H. Benaddi, T.J. Bandosz, J. Jagiello, J.A. Schwarz, J.N. Rouzaud, D. Legrasc, F. Béguina, Surface functionality and porosity of activated carbons obtained from chemical activation of wood, Carbon 38 (2000) 669–674.

[21] R.W. Gaikwad, S.A.M. Kinldy, Studies on auramine dye adsorption on psidium guava leaves, Korean J. Chem. Eng. 26 (2009) 102.

[22] E. Demirbas, M. Kobyab, E. Senturkb, T. Ozkana, Adsorption kinetics for the removal of chromium (VI) from aqueous solutions on the activated carbons prepared from agricultural wastes, Gebze Institute of Technology, 41400 Gebze, Turkey, 2004.

[23] R. Ahmad, R. Kumar, Adsorption studies of hazardous malachite green onto treated ginger waste, J. Environ. Manage. 91 (2010) 1032.
[24] M.M. El-Halwany, Study of adsorption isotherms and kinetic models for methylene blue adsorption on activated carbon developed from Egyptian rice hull (Part II), Desalination 250 (2010) 208.
[25] E. Demirbas, M. Kobya, M.S. Oncel, S. Sencan, Removal of Ni (II) from aqueous solution by adsorption onto hazelnut shell activated carbon: Equilibrium studies, Bioresour. Technol. 84 (2002) 291.
[26] M.M. El-Halwany, Thermodynamic functions and kinetic models for methelyne blue adsorption on corn straw pulp, Mansoura Eng. J. 34 (2009) 15.
[27] T.E. Farrag, M.M. El-Halwany, Kinetic models for methylene blue adsorption using activated human hair waste as a biosorbent, Alexanderia Eng. J. 48 (2009) 355.
[28] M.-H. Baek, C.O. Ijagbemi, O. Se-Jin, D.-S. Kim, Removal of Malachite Green from aqueous solution using degreased coffee bean, J. Hazard. Mater. 176 (2010) 820.
[29] V.K. Garg, R. Gupta, A.B. Yadav, R. Kumar, Dye removal from aqueous solution by adsorption on treated sawdust, Bioresour. Technol. 89 (2003) 121.
[30] J. Zhang, Y. Li, C. Zhang, Y. Jing, Adsorption of Malachite Green from aqueous solution onto carbon prepared from Arundo donax root, J. Hazard. Mater. 150 (2008) 774.
[31] M.J. Iqbal, M.N. Ashiq, Adsorption of dyes from aqueous solutions on activated charcoal, J. Hazard. Mater. B139 (2007) 57.
[32] C.A. Basar, Applicability of the various adsorption models of three dyes adsorption onto activated carbon prepared apricot, J. Hazard. Mater. B135 (2006) 232.
[33] I.D. Mall, V.C. Srivastava, N.K. Agarwal, I.M. Mishra, Adsorptive removal of Malachite Green dye from aqueous solution by bagasse fly ash and activated carbon-kinetic study and equilibrium isotherm analyses, Colloids Surf. A 264 (2005) 17.
[34] S.S. Tahir, N. Rauf, Removal of a cationic dye from aqueous solutions by adsorption onto bentonite clay, Chemosphere 63 (2006) 1842.
[35] S.D. Khattri, M.K. Singh, Colour removal from dye wastewater using sugar cane dust as an adsorbent, Adsorpt. Sci. Technol. 17 (1999) 269.
[36] A. Mittal, Adsorption kinetics of removal of a toxic dye. Malachite Green, from wastewater by using hen feathers, J. Hazard. Mater. B133 (2006) 196.
[37] P. Janos, Sorption of basic dyes onto iron humate, Environ. Sci. Technol. 37 (2003) 5792.
[38] K.V. Kumar, S. Sivanesan, Isotherms for Malachite Green onto rubber wood (Hevea brasiliensis) sawdust: Comparison of linear and non-linear methods, Dyes Pigments 72 (2007) 124.
[39] C.P. Sekhar, S. Kalidhasan, V. Rajesh, N. Rajesh, Bio-polymer adsorbent for the removal of Malachite Green from aqueous solution, Chemosphere 77 (2009) 842.
[40] K.G. Bhattacharyya, A. Sarma, Adsorption characteristics of the dye, brilliant green, on neem leaf powder, Dyes Pigments 57 (2003) 211.
[41] T. Santhi, S. Manonmani, T. Smitha, Removal of Malachite Green from aqueous solution by activated carbon prepared from the epicarp of *Ricinus communis* by adsorption, J. Hazard. Mater. 179 (2010) 178.
[42] K.V. Kumar, Optimum sorption isotherm by linear and non-linear methods for Malachite Green onto lemon peel, Dyes Pigments 74 (2007) 595.
[43] Z. Bekci, Y. Seki, L. Cavas, Removal of Malachite Green by using an invasive marine alga *Caulerpa racemosa* var. cylindracea, J. Hazard. Mater. 161 (2009) 1454.
[44] B.H. Hameed, M.I. El-Khaiary, Malachite Green adsorption by rattan sawdust: Isotherm, kinetic and mechanism modeling, J. Hazard. Mater. 159 (2008) 574.
[45] G.H. Sonawane, V.S. Shrivastava, Kinetics of decolourization of Malachite Green from aqueous medium by maize cob (Zea maize): An agricultural solid waste, Desalination 247 (2009) 430.